

Impaired Insulin Signaling in Endothelial Cells Reduces Insulin-Induced Glucose Uptake by Skeletal Muscle

Tetsuya Kubota,^{1,3,5,18} Naoto Kubota,^{1,3,6,18,*} Hiroki Kumagai,^{1,18} Shinichi Yamaguchi,¹ Hideki Kozono,¹ Takehiro Takahashi,¹ Mariko Inoue,^{1,3} Shinsuke Itoh,¹ Iseki Takamoto,^{1,6} Takayoshi Sasako,¹ Katsuyoshi Kumagai,^{1,6} Tomoko Kawai,^{1,3} Shinji Hashimoto,¹ Tsuneo Kobayashi,⁷ Maki Sato,⁸ Kumpei Tokuyama,⁸ Satoshi Nishimura,² Masaki Tsunoda,⁹ Tomohiro Ide,⁹ Koji Murakami,⁹ Tomomi Yamazaki,⁴ Osamu Ezaki,⁴ Koichi Kawamura,¹⁰ Hirotake Masuda,¹⁰ Masao Moroi,⁵ Kaoru Sugi,⁵ Yuichi Oike,¹¹ Hiroaki Shimokawa,¹² Nobuyuki Yanagihara,¹³ Masato Tsutsui,¹⁴ Yasuo Terauchi,¹⁵ Kazuyuki Tobe,¹⁶ Ryozo Nagai,^{2,6} Katsuo Kamata,⁷ Kenji Inoue,¹⁷ Tatsuhiko Kodama,^{6,17} Kohjiro Ueki,^{1,6} and Takashi Kadowaki^{1,3,6,*}

¹Department of Diabetes and Metabolic Diseases

²Department of Cardiovascular Diseases

Graduate School of Medicine, University of Tokyo, Tokyo 113-8655, Japan

³Clinical Nutrition Program

⁴Nutritional Science Program

National Institute of Health and Nutrition, Tokyo 162-8636, Japan

⁵Division of Cardiovascular Medicine, Toho University Ohashi Medical Center, Tokyo 113-8655, Japan

⁶Translational Systems Biology and Medicine Initiative, University of Tokyo, Tokyo 153-8515, Japan

⁷Department of Physiology and Morphology, Institute of Medicinal Chemistry, Hoshi University, Tokyo 142-8501, Japan

⁸Graduate School of Comprehensive Human Science, University of Tsukuba, Tsukuba 305-8577, Japan

⁹Bioscience Division 1, Metabolic Discovery Research Laboratories, Kyorin Pharmaceutical Co. Ltd., Shimotsuga 329-0014, Japan

¹⁰Second Department of Pathology, Akita University School of Medicine, Akita 010-8543, Japan

¹¹Department of Molecular Genetics, Graduate School of Medical Sciences, Kumamoto University, Kumamoto 860-8556, Japan

¹²Department of Cardiovascular Medicine, Tohoku University Graduate School of Medicine, Sendai 980-8574, Japan

¹³Department of Pharmacology, University of Occupational and Environmental Health, School of Medicine, Kitakyushu 807-8555, Japan

¹⁴Department of Pharmacology, Faculty of Medicine, University of the Ryukyus, Okinawa 903-0215, Japan

¹⁵Department of Diabetes and Endocrinology, Yokohama City University, School of Medicine, Kanagawa 236-0004, Japan

¹⁶First Department of Internal Medicine, Faculty of Medicine, University of Toyama, Toyama, 930-0194, Japan

¹⁷Laboratory for Systems Biology and Medicine, Research Center for Advanced Science and Technology, University of Tokyo, Tokyo 153-8904, Japan

¹⁸These authors contributed equally to this work

*Correspondence: kadowaki-3im@h.u-tokyo.ac.jp (T.K.), nkubota-ty@umin.ac.jp (N.K.)

DOI 10.1016/j.cmet.2011.01.018

SUMMARY

In obese patients with type 2 diabetes, insulin delivery to and insulin-dependent glucose uptake by skeletal muscle are delayed and impaired. The mechanisms underlying the delay and impairment are unclear. We demonstrate that impaired insulin signaling in endothelial cells, due to reduced *Irs2* expression and insulin-induced eNOS phosphorylation, causes attenuation of insulin-induced capillary recruitment and insulin delivery, which in turn reduces glucose uptake by skeletal muscle. Moreover, restoration of insulin-induced eNOS phosphorylation in endothelial cells completely reverses the reduction in capillary recruitment and insulin delivery in tissue-specific knockout mice lacking *Irs2* in endothelial cells and fed a high-fat diet. As a result, glucose uptake by skeletal muscle is restored in these mice. Taken together, our results show that insulin signaling in endothelial cells plays a pivotal role in the regulation of glucose uptake by skeletal

muscle. Furthermore, improving endothelial insulin signaling may serve as a therapeutic strategy for ameliorating skeletal muscle insulin resistance.

INTRODUCTION

Skeletal muscle is one of the major target organs of insulin actions and plays an essential role in insulin-induced glucose uptake (DeFronzo et al., 1979; Bergman, 1989). Insulin, secreted by the pancreatic β cells, is delivered into the capillaries and crosses the endothelial barrier to enter the interstitial spaces (Vincent et al., 2005). It then binds to the insulin receptors on the skeletal muscle cell surface, activating intracellular pathways in the skeletal muscle (White and Kahn, 1994; Petersen et al., 2004; Long and Zierath, 2008). Recent evidence indicates that insulin delivery to the skeletal muscle interstitium is the rate-limiting step in insulin-stimulated glucose uptake by the skeletal muscle, and is much slower in obese insulin-resistant subjects than in normal subjects (Sherwin et al., 1974; DeFronzo et al., 1979; Yang et al., 1989; Jansson et al., 1993; Miles et al., 1995; Sjostrand et al., 2002; Barrett et al., 2009). Andres and colleagues have shown that insulin is distributed more slowly

to the compartment corresponding to the skeletal muscle than to other compartments, and the time course of insulin equilibration with this pool closely paralleled the glucose infusion rate (GIR) in their compartmental model (Sherwin et al., 1974; DeFronzo et al., 1979). Moreover, the dynamics of insulin concentrations in the skeletal muscle lymphatics, which is derived from the interstitial fluid in the skeletal muscle, is actually slow, and is significantly correlated with the peripheral glucose uptake after insulin infusion (Yang et al., 1989). In obese subjects, the appearance of insulin in the interstitial fluid of the skeletal muscle and onset of insulin action after insulin infusion were found to be significantly delayed in comparison with the results in control subjects (Sjostrand et al., 2002). Although the slow onset of insulin action on glucose disposal *in vivo* could be secondary to a slow response by the cellular machinery within the myocytes, which are the cells responsible for glucose uptake in the skeletal muscle, insulin-induced glucose uptake by myocytes *in vitro* appears to be fully activated within 2–5 min, much earlier than that *in vivo* (Karnieli et al., 1981). Moreover, Bergman et al. demonstrated that injection of insulin directly into the interstitium of the skeletal muscle is followed by a prompt increase in the glucose uptake (Chiu et al., 2008). Based on these findings, insulin delivery may determine the *in vivo* time course of insulin-induced glucose uptake, which may be much slower than the insulin-induced glucose uptake *in vitro*.

Two discrete steps have been reported to increase insulin delivery to the skeletal muscle: an increase in the available capillary surface area (capillary recruitment), and an increase in the transendothelial transport of insulin. Clark and colleagues measured capillary recruitment following insulin infusion and found that it was associated with increased glucose uptake by the skeletal muscle (Rattigan et al., 1997; Vincent et al., 2004). The insulin-induced capillary recruitment and glucose uptake were reported to be significantly impaired in obese subjects and diabetic models (Wallis et al., 2002; Keske et al., 2009). In addition to the vasoactive actions of insulin on the capillaries, insulin may promote its own movement across the endothelial barrier. Recent *in vivo* evidence suggests that transendothelial transport of insulin in the skeletal muscle increased along with elevation of the plasma insulin levels, and that these levels were diminished in the presence of high-fat (HF) diet-induced insulin resistance (Hamilton-Wessler et al., 2002; Ellmerer et al., 2006; Wang et al., 2008). It is still unclear whether capillary recruitment and transendothelial transport of insulin may be related or may function independently (Clark, 2008).

We hypothesized that an insulin signaling defect in the endothelial cells impairs insulin-induced capillary recruitment and insulin delivery in the skeletal muscle in obesity. In HF diet-fed obese mice, the expression levels of insulin receptor substrate (Irs)2, which is the major Irs isoform expressed in the endothelial cells (Kubota et al., 2003), were markedly reduced, and insulin-induced eNOS phosphorylation, capillary recruitment, and insulin delivery were markedly impaired. Consistent with these results, mice with Irs2 deletion in the endothelial cells (ETIrs2KO mice) also exhibited a reduction of insulin-induced eNOS phosphorylation, capillary recruitment, and insulin delivery. Moreover, restoration of the insulin-induced eNOS phosphorylation in the endothelial cells completely reversed the reduction of the capillary recruitment and insulin delivery in both the HF diet-

fed and ETIrs2KO mice. We conclude that a genetically and/or environmentally induced insulin signaling defect in the endothelial cells causes skeletal muscle insulin resistance as a consequence of the impaired insulin-induced capillary recruitment and insulin delivery.

RESULTS

Insulin Signaling Was Significantly Impaired in the Endothelial Cells of the ob/ob and HF Diet-Fed Mice

To investigate insulin signaling in the endothelial cells in mouse models of obesity, we first measured the expression levels of the insulin receptor (I_r) and I_r substrate (I_{rs}) in mice with genetically (ob/ob mice) or environmentally induced (8-week HF diet-fed mice) obesity. Although there were no significant differences in the mRNA or protein expression levels of I_r and endothelin (ET)-1 (see Figures S1A and S1B available online), the mRNA and protein expression levels of I_{rs}1 were reduced by approximately 50% and those of I_{rs}2, the major I_{rs} isoform expressed on the endothelial cells (Kubota et al., 2003), by approximately 80% in the endothelial cells of both the mouse models of obesity (Figures 1A and 1B). To elucidate the mechanisms by which the expressions of I_{rs}1 and I_{rs}2 in the endothelial cells were downregulated, we investigated the effects of FFA on the expressions of I_{rs}1 and I_{rs}2 following continuous administration of intralipid for 24 hr in C57Bl/6 mice. Although a 7-fold increase of the plasma FFA levels was observed after the intralipid treatment, the expression levels of I_{rs}1 and I_{rs}2 measured before and after the intralipid treatment were not significantly different (Figure S1C). We next investigated whether the I_{rs}1 and I_{rs}2 gene expressions in the endothelial cells might be altered by hyperinsulinemia induced by continuous administration of insulin for 24 hr using a miniosmotic pump in C57Bl/6 mice. After continuous administration of insulin for 24 hr, a 7-fold increase of the plasma insulin levels was noted (Figure 1C). In regard to the expression levels of the I_{rs}1 and I_{rs}2, on the other hand, while no change in the expression of endothelial I_{rs}1 was observed, the expression of endothelial I_{rs}2 was significantly decreased (Figure 1C). These data suggest that hyperinsulinemia may be one of the mechanisms underlying the decrease in the expression of endothelial I_{rs}2 observed in the ob/ob and HF diet-fed mice, although the reason for the downregulated I_{rs}1 expression in these mice still remains unexplained. The insulin signaling cascade activates Akt, which in turn phosphorylates and activates eNOS in the endothelial cells (Muniyappa and Quon, 2007). Consistent with the results for the expression levels of I_{rs}1 and I_{rs}2, insulin-stimulated phosphorylations of Akt and eNOS were decreased by 70%–80% in the endothelial cells of the ob/ob and HF diet-fed mice (Figure 1D), indicating that insulin signaling was impaired in the endothelial cells of these obesity models. We then investigated whether impaired insulin signaling in the endothelial cells might be involved in the HF diet-induced, obesity-linked impairment of glucose uptake by the skeletal muscle. Although an increase of the capillary blood volume at 10 min after the insulin infusion in the hyperinsulinemic-euglycemic clamp study was observed in the normal chow-fed mice, no such increase was observed in the HF diet-fed mice (Figure 1E). On the other hand, no increase of

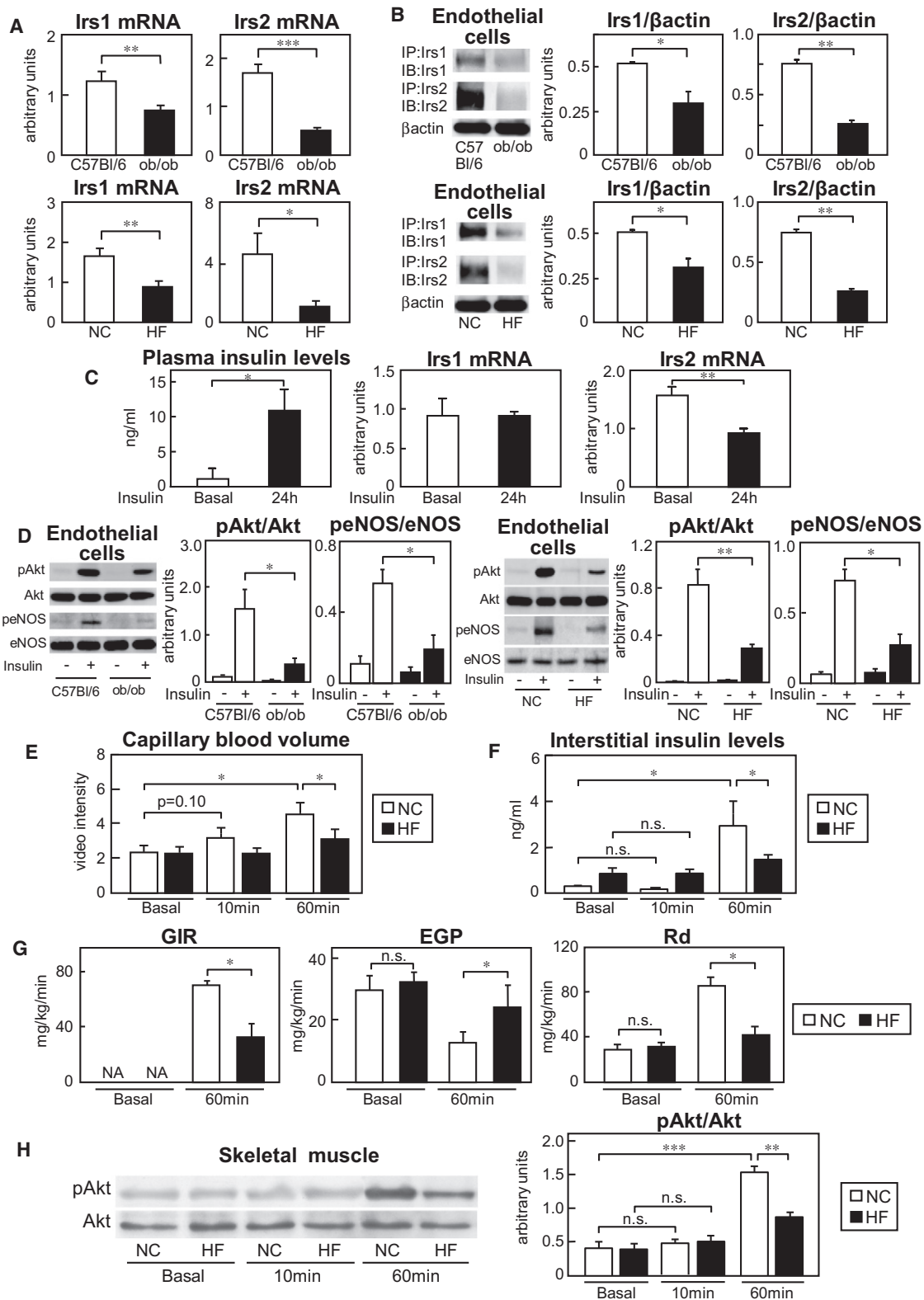


Figure 1. In the HF Diet-Fed Obese Mice, which Show Impaired Glucose Uptake by the Skeletal Muscle, Decreased Insulin-Induced Phosphorylation of eNOS in the Endothelial Cells, along with Downregulation, Mainly of Irs2, Was Associated with Attenuation of the Insulin-Induced Increase of the Capillary Blood Volume and of the Increase of the Interstitial Concentrations of Insulin

(A and B) Expression levels of Irs1 or Irs2 mRNA and protein in the endothelial cells of the ob/ob and HF diet-fed mice (n = 3–11).

the interstitial concentrations of insulin was observed at 10 min after the insulin infusion in either the normal chow-fed or the HF diet-fed mice (Figure 1F). These data suggest that capillary recruitment starts to increase well before the increase of the interstitial insulin concentrations, consistent with the results of previous studies (Miles et al., 1995; Vincent et al., 2005). Insulin-induced increases of the capillary blood volume and interstitial concentrations of insulin were significantly impaired at 60 and 120 min after the insulin infusion in the hyperinsulinemic-euglycemic clamp study (Figures 1E and 1F; Movies S1A and S1B, and data not shown), even when the plasma insulin levels were adjusted to be the same in both the normal chow-fed and HF diet-fed mice (Figure S1D and data not shown). A significant decrease of the GIR and glucose disappearance rate (Rd), as also a significant increase of the endogenous glucose production (EGP), were found in the animals at 60 and 120 min after the insulin infusion in the hyperinsulinemic-euglycemic clamp study (Figure 1G and data not shown). Consistent with these results, the phosphorylation levels of Akt in the skeletal muscle in the normal chow-fed mice began to increase by 30 min and reached its peak about 60 min after the insulin infusion, whereas this increase of the Akt phosphorylation level from 30 min onward after the insulin infusion in the hyperinsulinemic-euglycemic clamp study was significantly impaired in the HF diet-fed mice (Figure 1H; Figure S1E and data not shown). These data suggest that the decreased phosphorylation level of eNOS induced by insulin in the endothelial cells associated with downregulation, mainly of Irs2, appears to be involved, along with the impaired insulin-induced capillary recruitment and increase of the interstitial concentrations of insulin, in the impaired glucose uptake by the skeletal muscle in the HF diet-fed obese mice.

ETIrs2KO Mice Exhibited Impaired Insulin-Induced Glucose Uptake by the Skeletal Muscle

In order to elucidate the causal relationship between insulin signaling in the endothelial cells and the glucose uptake by the skeletal muscle, we generated ETIrs2KO mice. The endothelial Irs2 mRNA levels were reduced by approximately 95% in the ETIrs2KO mice, whereas the Irs2 expression levels in the white adipose tissue (WAT), liver, and skeletal muscle remained unchanged (Figures 2A and 2B). The Irs2 protein expression and insulin-stimulated tyrosine phosphorylation of Irs2 were almost completely abrogated in the endothelial cells of the ETIrs2KO mice (Figure 2C). There were no significant differences in the mRNA and protein levels of eNOS or ET-1 between the control and ETIrs2KO mice (Figures S2A and S2B). The basal blood glucose and plasma insulin levels were indistinguishable between the control and ETIrs2KO mice (Figure S2C). Insulin-stimulated phosphorylations of Akt and eNOS were found to be significantly reduced in the endothelial cells of the ETIrs2KO

mice (Figure 2D). Although an increase of the capillary blood volume was observed in the control mice by 10 min after the insulin infusion in the hyperinsulinemic-euglycemic clamp study, no such increase was observed in the ETIrs2KO mice (Figure 2E). In contrast, no increase in the interstitial concentrations of insulin was observed at 10 min after the insulin infusion in either the control or the ETIrs2KO mice (Figure 2F). The insulin-induced increases of the capillary blood volume and interstitial concentrations of insulin were significantly impaired at 60 and 120 min after insulin infusion in the hyperinsulinemic-euglycemic clamp study (Figures 2E and 2F and data not shown), even when the plasma insulin levels were adjusted to be the same in both the control and ETIrs2KO mice (Figure S2D and data not shown). Furthermore, the whole-body insulin sensitivity and glucose tolerance were also significantly impaired in the ETIrs2KO mice (Figures 2G and 2H). The GIR and Rd at 60 and 120 min after insulin infusion in the hyperinsulinemic-euglycemic clamp study were significantly reduced in the ETIrs2KO mice (Figure 2I and data not shown). The decreased Rd observed in the ETIrs2KO mice during the hyperinsulinemic-euglycemic clamp, however, indicates impairment of glucose uptake by mainly the skeletal muscle, but also by other tissues containing nonfenestrated endothelial cells forming tight junctions. Thus, we also measured the insulin-induced glucose uptake by the skeletal muscle during the hyperinsulinemic-euglycemic clamp study using 2-deoxy- ^3H glucose (2- ^3H DG). Consistent with the results obtained for the Rd, the skeletal muscle glucose uptake was significantly reduced in the ETIrs2KO mice (Figure 2J), suggesting that the glucose uptake through the capillaries, at least, was impaired in the skeletal muscle of the ETIrs2KO mice. In contrast, glucose uptake by the isolated skeletal muscle from the ETIrs2KO mice was not impaired (Figure 2K), indicating that glucose uptake by the skeletal muscle per se was not impaired in the ETIrs2KO mice. Consistent with these results, the phosphorylation level of Akt in the skeletal muscle in the control mice began to increase by 30 min and reached its peak about 60 min after insulin infusion in the hyperinsulinemic-euglycemic clamp study, whereas this increase in the Akt phosphorylation level was significantly impaired in the ETIrs2KO mice (Figure 2L; Figure S2E and data not shown). Moreover, the phosphorylation levels of Irf β , as well as those of Irs1 and Akt, in the skeletal muscle were also significantly decreased in the ETIrs2KO mice at 60 min after insulin infusion into the inferior vena cava (Figure S2F). In contrast, no significant differences in the phosphorylation levels of Irf β , Irs1, Irs2, or Akt in the liver were observed between the control and ETIrs2KO mice (Figure S2G), even though Irs2 was also deleted from the hepatic endothelial cells of the ETIrs2KO mice (Figure S2H). Quantitative analysis revealed no significant difference in the β cell mass between the control and ETIrs2KO mice (Figure S2I). These data suggest that Irs2 deletion in the endothelial cells causes an insulin

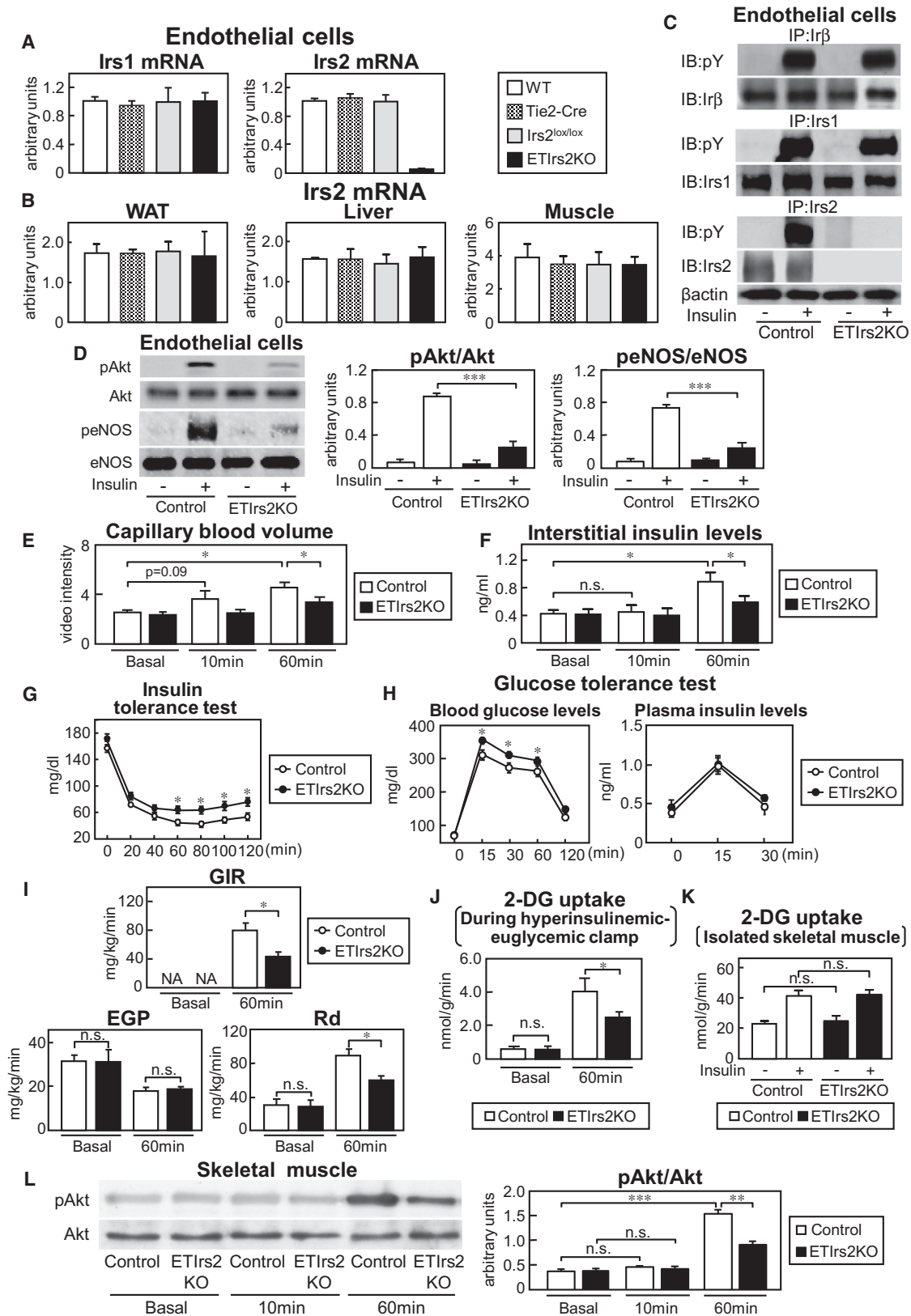
(C) Expression levels of Irs1 and Irs2 mRNA after insulin infusion (n = 3–4).

(D) Phosphorylation levels of Akt and eNOS in the ob/ob and HF diet-fed mice (n = 4–7).

(E and F) Capillary blood volume (E) and interstitial insulin levels (F) in the HF diet-fed mice (n = 3–10).

(G) GIR, EGP, and Rd in the HF diet-fed mice after insulin infusion in the hyperinsulinemic-euglycemic clamp study (n = 7–9).

(H) Phosphorylation levels of Akt (ser473) in the skeletal muscle of the HF diet-fed mice after insulin infusion in the hyperinsulinemic-euglycemic clamp study (n = 3–4). “NC” indicates normal chow-fed mice. “NA” indicates not applicable. Where error bars are shown, the results represent the means \pm SEM. *p < 0.05, **p < 0.01, ***p < 0.001.



signaling defect in the cells that results in impairment of insulin-induced eNOS phosphorylation, capillary recruitment, and increase of the interstitial concentrations of insulin, consequently impairing the skeletal muscle glucose uptake.

Insulin-Induced Glucose Uptake by the Skeletal Muscle Was Not Impaired in the ETIrs1KO Mice, but Was Significantly Reduced in the ETIrs1/2DKO Mice, as Compared with that in the ETIrs2KO Mice

To investigate the role of *Irs1* expressed in the endothelial cells in the regulation of insulin-induced glucose uptake by the skeletal muscle, we generated mice with endothelial-cell-specific *Irs1* knockout (ETIrs1KO mice). Although the *Irs1* mRNA and protein levels were almost completely abrogated in the endothelial cells of the ETIrs1KO mice (Figures 3A and 3B), no significant differences in the expression levels of *Irs2*, eNOS, or ET-1 mRNA and protein were observed between the control and ETIrs1KO mice (Figures 3A and 3B). No significant difference in the insulin-stimulated phosphorylation levels of Akt or eNOS was observed between the control and ETIrs1KO mice (Figure 3C). Furthermore, no significant differences in the results of the insulin tolerance test or glucose tolerance test were observed between the control and ETIrs1KO mice (Figures 3D and 3E). Consistent with these results, there were also no significant differences in the results of the hyperinsulinemic-euglycemic clamp study between the control and ETIrs1KO mice (Figure 3F).

We next generated mice with endothelial-cell-specific *Irs1/Irs2* double-knockout (ETIrs1/2DKO), in an attempt to elucidate whether insulin signaling in the endothelial cells might be exclusively mediated by *Irs1* and *Irs2*. Although the *Irs1* and *Irs2* mRNA and protein levels were almost completely abrogated in the endothelial cells of the ETIrs1/2DKO mice (Figures 3G and 3H), no significant differences in the mRNA or protein levels of eNOS and ET-1 were observed between the control and ETIrs1/2DKO mice (Figures 3G and 3H). The insulin-stimulated phosphorylation levels of Akt and eNOS were significantly reduced in the ETIrs1/2DKO mice (Figure 3I). The insulin tolerance test revealed that the glucose-lowering effect of insulin was significantly attenuated in the ETIrs1/2DKO mice (Figure 3J), and the glucose tolerance test revealed significantly elevated plasma glucose levels in the ETIrs1/2DKO mice (Figure 3K). Moreover, the GIR and Rd in the ETIrs1/2DKO mice were significantly reduced as compared with the values not only in the

control mice but also in the ETIrs2KO mice (Figure 3L). These data suggest that *Irs1* may play a significant role in endothelial cell insulin signaling, which becomes evident especially when *Irs2* expression is downregulated, such as in the ETIrs2KO and HF diet-fed mice.

Restoration of Insulin-Induced eNOS Phosphorylation in the Endothelial Cells Restored Glucose Uptake by the Skeletal Muscle in the ETIrs2KO Mice

To determine whether restoration of the insulin-induced eNOS phosphorylation in the endothelial cells might restore the glucose uptake by the skeletal muscle, we administered beraprost sodium (BPS), a stable prostaglandin (PGI)₂ analog (Kainoh et al., 1991), to the ETIrs2KO mice; this agent has been reported to increase the expression levels of eNOS mRNA and protein through the cyclic adenosine monophosphate (cAMP)-, protein kinase A-, and cAMP-responsive element-mediated pathways (Niwano et al., 2003). Indeed, this treatment increased the eNOS mRNA and protein expression levels in the endothelial cells (Figures 4A and 4B). BPS treatment restored insulin-induced phosphorylation of eNOS in the BPS-treated ETIrs2KO mice to a level similar to that observed in the saline-treated control mice (Figure 4B), despite the absence of any change in the ratio of phosphorylated eNOS to total eNOS (Figure 4B); also, no change in the insulin-induced phosphorylation of Akt was observed in these mice (Figure S3A). The insulin-induced increase of the capillary blood volume and interstitial concentrations of insulin were restored at 60 and 120 min after insulin infusion in the hyperinsulinemic-euglycemic clamp study (Figures 4C and 4D and data not shown) under comparable plasma insulin concentrations (Figure S3B and data not shown). The restoration of the insulin-induced increase of the capillary blood volume by BPS treatment in the ETIrs2KO mice was completely blocked by administration of the NOS inhibitor, N^G-nitro-L-arginine methyl ester (L-NAME) (Figure 4E), suggesting that the restoration of the insulin-induced capillary recruitment by BPS treatment was eNOS dependent. To rule out the possibility that BPS and L-NAME regulated the skeletal muscle glucose uptake through an eNOS-independent mechanism, we next administered BPS and L-NAME to eNOS-knockout (eNOSKO) mice. There were no significant differences in the insulin-induced increases of the capillary blood volume or interstitial insulin concentrations among the saline-treated, BPS-treated, and L-NAME-treated eNOSKO mice, either at the basal

Figure 2. *Irs2* Deletion in the Endothelial Cells Caused an Insulin Signaling Defect Resulting in a Reduction of the Insulin-Induced Increase of the Capillary Blood Volume and Interstitial Concentrations of Insulin and, as a Consequence, Impaired Glucose Uptake by the Skeletal Muscle

- (A) Expression levels of *Irs1* and *Irs2* mRNA in the endothelial cells of the WT, Tie2-Cre, *Irs2lox/lox*, and ETIrs2KO mice (n = 4–8).
 (B) The expression levels of *Irs2* in the WAT, liver, and skeletal muscle of the WT, Tie2-Cre, *Irs2lox/lox*, and ETIrs2KO mice (n = 5–6).
 (C) Insulin-stimulated tyrosine phosphorylation levels of *Irf3*, *Irs1*, and *Irs2* in the endothelial cells of the ETIrs2KO mice.
 (D) Phosphorylation levels of Akt and eNOS in the endothelial cells of the ETIrs2KO mice (n = 8–12).
 (E and F) Capillary blood volume (E) and interstitial insulin levels (F) in the ETIrs2KO mice (n = 3–10).
 (G and H) Insulin tolerance test (G) and glucose tolerance test (H) in the ETIrs2KO mice (n = 8–10).
 (I) GIR, EGP, and Rd in the ETIrs2KO mice after insulin infusion in the hyperinsulinemic-euglycemic clamp study (n = 3–9).
 (J) Glucose uptake by the skeletal muscle in the ETIrs2KO mice after insulin infusion in the hyperinsulinemic-euglycemic clamp study (n = 3–9).
 (K) Glucose uptake by the isolated skeletal muscle in the ETIrs2KO mice (n = 3).
 (L) Phosphorylation levels of Akt (ser473) in the skeletal muscle of the ETIrs2KO mice after insulin infusion in the hyperinsulinemic-euglycemic clamp study (n = 3–4). “Control” indicates *Irs2lox/lox* mice. “NA” indicates not applicable. Where error bars are shown, the results represent the means ± SEM. *p < 0.05, **p < 0.01, ***p < 0.001.

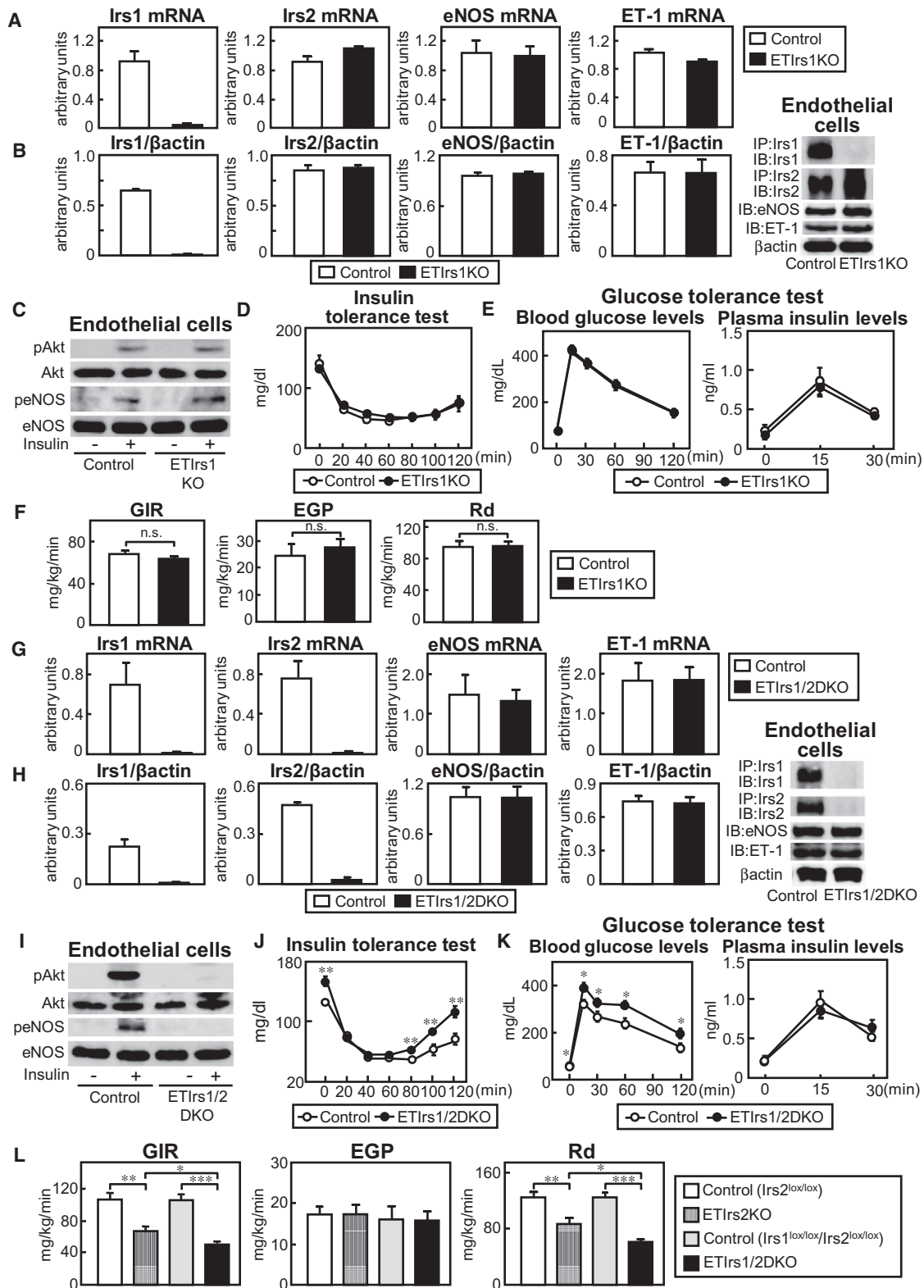


Figure 3. In the ETIrs1/2DKO, but Not ETIrs1KO, Mice, the GIR and Rd Were Significantly Reduced as Compared with the Values Seen Not Only in the Control Mice, But Also in the ETIrs2KO Mice, in Addition to the Impairment of Insulin Signaling in the Endothelial Cells, Whole-Body Insulin Sensitivity, and Glucose Tolerance

(A and B) Expression levels of *Irs1*, *Irs2*, eNOS, or ET-1 mRNA and protein in the endothelial cells of the ETIrs1KO mice (n = 3–6).

or at 60 min after insulin infusion (Figures S3C and S3D). Moreover, there were no significant differences in the results of the insulin tolerance or glucose tolerance tests, or in the skeletal muscle glucose uptake among the three groups (Figures S3E–S3G). These data strongly suggest that the effects of both BPS and L-NAME were eNOS dependent. The GIR and Rd were completely restored in the BPS-treated ETIrs2KO mice at 60 and 120 min after insulin infusion (Figure 4F and data not shown). We also measured the glucose uptake by the skeletal muscle after insulin infusion in the hyperinsulinemic-euglycemic clamp study. Glucose uptake by the skeletal muscle after insulin infusion was completely restored in the BPS-treated ETIrs2KO mice (Figure 4G). On the other hand, the glucose uptake by the isolated skeletal muscle from the BPS-treated ETIrs2KO mice remained essentially unchanged (Figure 4H), indicating the absence of any significant effect of BPS treatment on the glucose uptake by the skeletal muscle per se. Consistent with the results for the interstitial insulin concentrations, the phosphorylation levels of Irf β , as well as those of Irs1 and Akt, in the skeletal muscle were also completely restored in the BPS-treated ETIrs2KO mice at 60 min after insulin infusion into the inferior vena cava (Figure S3H). These data suggest that restoration of the insulin-induced phosphorylation of eNOS in the endothelial cells also restored the insulin-induced capillary recruitment and increase of the interstitial concentrations of insulin, consequently restoring the insulin-induced glucose uptake by the skeletal muscle. Alternatively, there is also the possibility that concomitant BPS plus insulin treatment activated eNOS via a pathway independent of the insulin/Irs/Akt pathway, even though BPS alone had no effect on eNOS phosphorylation. No significant differences were observed in the food intake, body weight, or weights of the visceral and subcutaneous fat pads among the three groups (Figure S4A). No significant differences in the plasma lipid profile or expression levels of adipokines were observed either among the three groups (Figures S4B and S4C). No significant difference in the 2-³H]DG uptake by the skeletal muscle was noted between the saline- and L-NAME-treated control mice (Figure S4D).

Restoration of Insulin-Induced eNOS Phosphorylation in the Endothelial Cells Restored the Glucose Uptake by the Skeletal Muscle in the HF Diet-Fed Mice

Could the restoration of insulin-induced eNOS phosphorylation in the endothelial cells also ameliorate the impaired glucose uptake by the skeletal muscle in the HF diet-fed obese mice? BPS treatment significantly increased the eNOS mRNA (Figure 5A) and protein (Figure 5B) expression levels. BPS treatment in the HF diet-fed mice restored insulin-induced phosphorylation of eNOS to a level similar to that observed in the saline-treated

normal chow-fed mice (Figure 5B), despite the absence of any change in the ratio of phosphorylated eNOS to total eNOS in the BPS-treated HF diet-fed mice (Figure 5B); also, no change in the insulin-induced phosphorylation of Akt was observed in these mice (Figure S5A). These data suggest that restoration of the insulin-induced eNOS phosphorylation in the BPS-treated HF diet-fed mice was not due to improvement of insulin signaling, but was rather proportional to the protein expression levels of eNOS. The decreased capillary blood volume and interstitial concentrations of insulin observed in the saline-treated HF diet-fed mice were restored at 60 and 120 min after insulin infusion in the BPS-treated HF diet-fed mice (Figures 5C and 5D and data not shown), when the plasma insulin levels were adjusted to be the same among the three groups (Figure S5B and data not shown). The restoration of the capillary blood volume by BPS treatment at 60 min after insulin infusion in the HF diet-fed mice was completely blocked by L-NAME treatment (Figure 5E). Consequently, the GIR and Rd at 60 and 120 min after insulin infusion were significantly, but not completely, restored by BPS treatment, although the increased EGP remained unchanged (Figure 5F and data not shown). We also measured the skeletal muscle glucose uptake after insulin infusion in the hyperinsulinemic-euglycemic clamp study. Glucose uptake by the skeletal muscle after insulin infusion was significantly, but not completely, restored in the BPS-treated HF diet-fed mice (Figure 5G). On the other hand, the glucose uptake by isolated skeletal muscle from the HF diet-fed mice treated with BPS remained essentially unchanged (Figure 5H), indicating the absence of any significant effect of BPS treatment on the glucose uptake by the skeletal muscle per se. Consistent with the results for the interstitial insulin concentrations, the insulin-induced phosphorylation levels of Irf β , as well as those of Irs1 and Akt, in the skeletal muscle at 60 min after insulin infusion into the inferior vena cava were significantly, but not completely, restored in the BPS-treated HF diet-fed mice (Figure S5C). Moreover, the increase in the blood glucose after glucose loading was significantly, but not completely, ameliorated during an oral glucose tolerance test conducted after BPS treatment in the HF diet-fed mice (Figure S5D). No significant differences in the food intake, body weight, or weights of the visceral and subcutaneous fat pads were noted between the saline- and BPS-treated HF diet-fed mice (Figure S5E). No significant differences in the plasma lipid profile or expression levels of adipokines were noted between the saline- and BPS-treated HF diet-fed mice (Figures S5F and S5G). Taken together, restoration of insulin-induced eNOS activation in the endothelial cells restored the insulin-induced capillary recruitment and interstitial insulin concentrations, resulting in improvement of the skeletal muscle glucose uptake in the HF diet-fed obese mice.

(C) Insulin-stimulated phosphorylation levels of Akt and eNOS in the endothelial cells of the ETIrs1KO mice (n = 3–5).

(D and E) Insulin tolerance test (D) and glucose tolerance test (E) in the ETIrs1KO mice (n = 6).

(F) GIR, EGP, and Rd in the ETIrs1KO mice during the hyperinsulinemic-euglycemic clamp study (n = 6–8).

(G and H) Expression levels of Irs1, Irs2, eNOS, and ET-1 mRNA and protein in the endothelial cells of the ETIrs1/2DKO mice (n = 3–6).

(I) Insulin-stimulated phosphorylation levels of Akt and eNOS in the endothelial cells of the ETIrs1/2DKO mice (n = 5–6).

(J and K) Insulin tolerance test (J) and glucose tolerance test (K) in the ETIrs1/2DKO mice (n = 8–9).

(L) GIR, EGP, and Rd in the ETIrs1/2DKO mice during the hyperinsulinemic-euglycemic clamp study (n = 5–10). “Control” of ETIrs1KO mice indicates Irs1^{lox/lox} mice; “Control” ETIrs1/2DKO mice indicates Irs1^{lox/lox}/Irs2^{lox/lox} mice. Where error bars are shown, the results represent the means \pm SEM. *p < 0.05, **p < 0.01, ***p < 0.001.

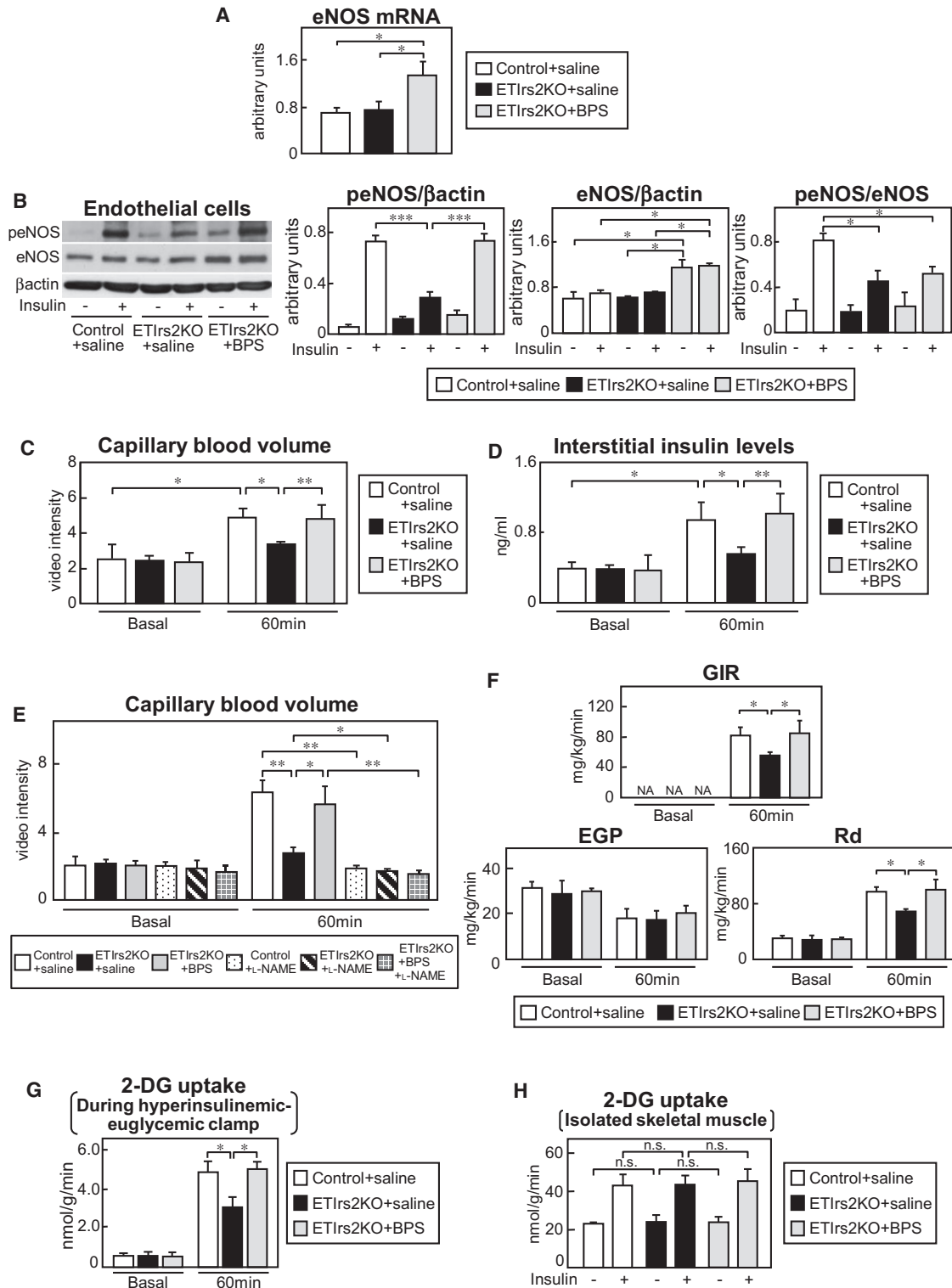


Figure 4. Restoration of the Insulin-Induced Phosphorylation of eNOS in the Endothelial Cells Restored the Insulin-Induced Increase of the Capillary Blood Volume and Interstitial Concentrations of Insulin; as a Consequence, the Insulin-Induced Glucose Uptake by the Skeletal Muscle Was Also Restored in the ETIrs2KO Mice

(A–D) eNOS mRNA levels (A), insulin-stimulated phosphorylation level of eNOS (B), capillary blood volume (C), and interstitial insulin concentrations (D) in the BPS-treated ETIrs2KO mice (n = 5–8).

(E) Capillary blood volume in the BPS-treated ETIrs2KO mice following L-NAME treatment (n = 4–6).

DISCUSSION

In this study, we demonstrated that endothelial insulin signaling is also significantly impaired in HF diet-fed mice, as in the other target organs of insulin, such as the liver and skeletal muscle. Moreover, insulin-induced capillary recruitment, increase of interstitial insulin concentrations, and glucose uptake were also significantly decreased in the skeletal muscle, all of which were reversed by restoration of the insulin-induced phosphorylation of eNOS in the endothelial cells. These data suggest that impaired insulin signaling in the endothelial cells, with reduction of *Irs2* expression and insulin-induced eNOS phosphorylation, reduces insulin-induced glucose uptake by the skeletal muscle via, at least in part, decreased capillary recruitment and decreased interstitial insulin concentrations in the skeletal muscle. In fact, an insulin signaling defect induced by *Irs2* deletion from the endothelial cells caused impaired insulin-induced glucose uptake by the skeletal muscle, along with attenuation of the insulin-induced capillary recruitment and increase of interstitial insulin concentrations.

Based on these data, we provide insight into the mechanism of insulin resistance in the skeletal muscle (Figure 6). Since the plasma insulin levels of lean subjects are low, and the expression levels of *Irs2* in their endothelial cells are presumably maintained under the fasting condition, insulin-mediated Akt and eNOS activations are induced optimally after feeding, resulting in insulin-induced capillary recruitment, increase of interstitial insulin concentrations, and increase of glucose uptake by the skeletal muscle. By contrast, since downregulation of *Irs2* expression is probably induced by hyperinsulinemia in the endothelial cells of obese subjects, the insulin-mediated Akt and eNOS activations after feeding are inadequate, and as a result, insulin-induced capillary recruitment, increase of interstitial insulin concentrations, and increase of glucose uptake by the skeletal muscle are impaired in obese subjects. This insight into the mechanism also sheds light on the physiological roles of *Irs2* in the endothelial cells. Expression of a sufficient amount of *Irs2* in the endothelial cells appears to be critical to normal glucose homeostasis. When *Irs2* expression is abundant in the fasting state, adequate glucose uptake by the skeletal muscle is induced and the elevated glucose levels return to within the normal range after feeding. However, when *Irs2* expression in the endothelial cells is reduced in the fasting state in the presence of hyperinsulinemia with insulin resistance, insulin signaling is impaired, and the elevated glucose levels after feeding fail to decrease efficiently, and in fact, the ETIrs2KO mice actually exhibited glucose intolerance in the glucose tolerance test (Figure 2H).

Insulin normally induces both vasorelaxation and vasoconstriction: insulin-induced vasorelaxation is mediated by the *Irs*-PI3K-Akt pathway increasing endothelial NO production, and insulin-induced vasoconstriction is mainly mediated by the *Shc*/SOS/Ras-MAPK pathway inducing ET-1 expression

(Muniyappa and Quon, 2007). While insulin-induced eNOS activation was significantly decreased in the endothelial cells of both the ETIrs2KO and ETIrs1/2DKO mice (Figures 2D and 3I), the ET-1 expressions remained unchanged in both models in this study, indicating that insulin signaling was selectively impaired in the endothelial cells of these mice (Figures 3G and 3H; Figures S2A and S2B). This selective insulin signaling defect appears to be critical to the impairment of the insulin-induced glucose uptake by the skeletal muscle. In fact, endothelial-cell-specific insulin receptor-knockout (VENIRKO) mice, in which both the *Irs*-PI3K-Akt-eNOS and *Shc*/SOS/Ras-MAPK-ET-1 pathways are disrupted, do not exhibit skeletal muscle insulin resistance (Vicent et al., 2003). Moreover, King et al. demonstrated that while the MAPK activity in the microvessels of obese Zucker rats remained unchanged, the *Irs1* protein and *Irs1*-associated PI3kinase activity were modestly reduced, and the *Irs2* protein and *Irs2*-associated PI3kinase activity were reduced even further (Jiang et al., 1999). Furthermore, VENIRKO mice developed insulin resistance when fed either low- or high-salt diets. These data suggest that the *Irs*-PI3K-Akt pathway may be more susceptible to the adverse effects of conditions such as obesity and dietary salt intake.

ETIrs2KO mice showed glucose intolerance, insulin resistance, and impaired glucose uptake by the skeletal muscle in vivo (Figures 2G–2J), despite the skeletal muscle per se not showing impaired insulin-induced glucose uptake (Figure 2K). In contrast, although myocyte-specific insulin receptor-knockout mice exhibited impaired glucose uptake by the skeletal muscle per se, as glucose uptake by insulin was decreased in the isolated skeletal muscle, the glucose tolerance and insulin sensitivity were almost normal in vivo (Brüning et al., 1998). Why did the ETIrs2KO, but not MIRKO, mice show skeletal muscle insulin resistance in vivo? It has been reported that there are mainly two different pathways of physiological glucose uptake by the skeletal muscle: one mediated in an insulin-dependent manner, such as after a meal, and the other in an insulin-independent manner, such as during exercise (Clark, 2008). Considering the phenotype of the MIRKO mice, the glucose uptake in the myocytes showing defective expression of the insulin receptor throughout growth and development may be largely compensated for by insulin-receptor-independent glucose uptake mechanisms. There may be little such compensatory mechanisms for glucose uptake in the ETIrs2KO mice, which show adequate expression of the insulin receptor in the skeletal muscle. Consequently, these mice may exhibit impairment of insulin-induced glucose uptake by the skeletal muscle, unlike the MIRKO mice.

To what degree is the impaired insulin delivery induced by the endothelial insulin signaling defect involved in the skeletal muscle insulin resistance in obesity and type 2 diabetes? Glucose uptake by the skeletal muscle was restored by 50% or more with improvement of the endothelial insulin signaling and insulin delivery in HF diet-fed mice (Figures 5B and 5G).

(F) GIR, EGP, and Rd in the BPS-treated ETIrs2KO mice after insulin infusion in the hyperinsulinemic-euglycemic clamp study ($n = 4-8$).

(G) Glucose uptake by the skeletal muscle in the BPS-treated ETIrs2KO mice after insulin infusion in the hyperinsulinemic-euglycemic clamp study ($n = 4-8$).

(H) Glucose uptake by the isolated skeletal muscle in the BPS-treated ETIrs2KO mice ($n = 3-6$). "NA" indicates not applicable. Where error bars are shown, the results represent the means \pm SEM. * $p < 0.05$, ** $p < 0.01$, *** $p < 0.001$.

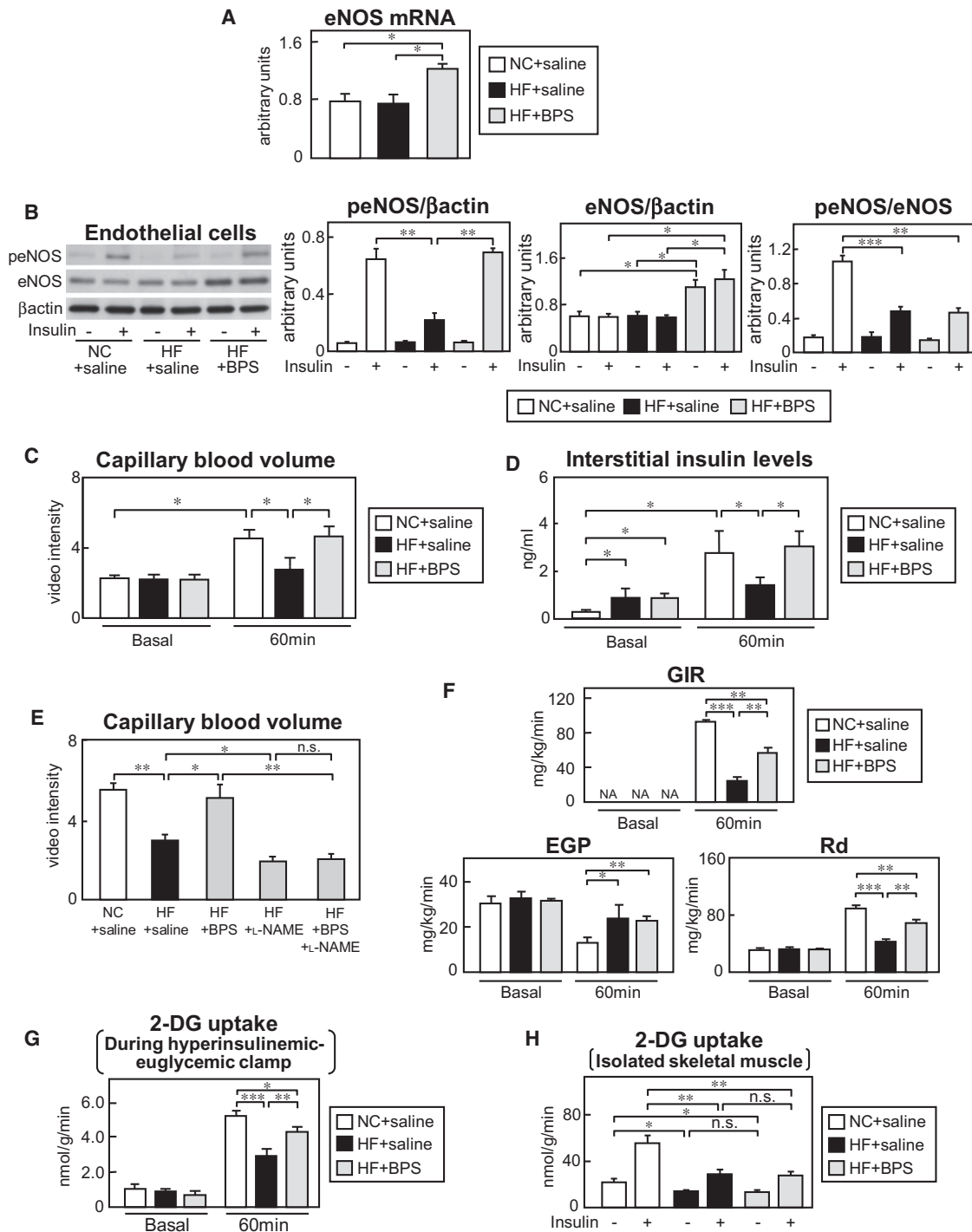


Figure 5. Restoration of the Insulin-Induced Phosphorylation of eNOS Restored the Insulin-Induced Increase of the Capillary Blood Volume and Interstitial Insulin Concentrations, Resulting in Improvement of the Glucose Uptake by the Skeletal Muscle in the HF Diet-Fed Obese Mice

(A–D) eNOS mRNA levels in the endothelial cells (A), insulin-stimulated phosphorylation level of eNOS (B), capillary blood volume (C), and interstitial insulin concentrations (D) in the BPS-treated HF diet-fed mice (n = 5–8).

(E) Capillary blood volume in the BPS-treated HF diet-fed mice following L-NAME treatment (n = 4–6).

(F) GIR, EGP, and Rd in the BPS-treated HF diet-fed mice after insulin infusion in the hyperinsulinemic-euglycemic clamp study (n = 3–5).

(G) Glucose uptake by the skeletal muscle in the BPS-treated HF diet-fed mice after insulin infusion in the hyperinsulinemic-euglycemic clamp study (n = 3–5).

(H) Glucose uptake by the isolated skeletal muscle in the BPS-treated HF diet-fed mice (n = 3–5). “NC” indicates normal chow-fed mice. “NA” indicates not applicable. Where error bars are shown, the results represent the means ± SEM. *p < 0.05, **p < 0.01, ***p < 0.001.

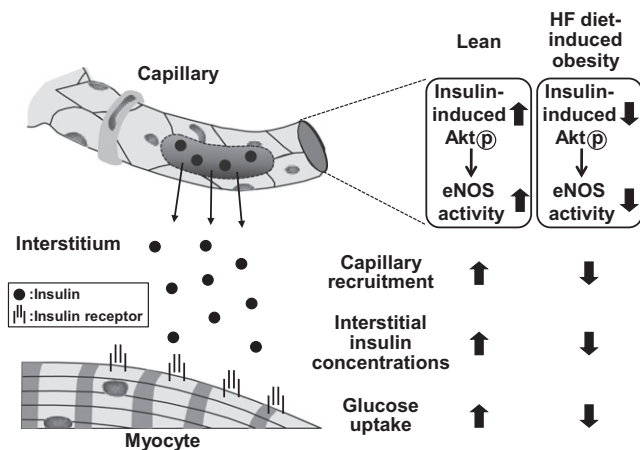


Figure 6. Impaired Insulin Signaling in the Endothelial Cells Reduces Insulin-Induced Glucose Uptake by the Skeletal Muscle in Obese Subjects

In lean subjects, the insulin-mediated Akt and eNOS activations are induced optimally in the endothelial cells after feeding, resulting in insulin-induced capillary recruitment, increase of interstitial insulin concentrations, and increase of the glucose uptake by the skeletal muscle. By contrast, since the insulin-mediated Akt and eNOS activations are inadequate in the endothelial cells of obese subjects after feeding, the insulin-induced capillary recruitment, increase or interstitial insulin concentrations, and increase of glucose uptake by the skeletal muscle are impaired.

Moreover, insulin delivery into the interstitial fluid is known to be delayed in insulin resistance (Sjostrand et al., 2002), as also is the onset of insulin stimulation of glucose uptake (Nolan et al., 1997). In addition, delivery of insulin, a molecule whose molecular weight is similar to that of insulin, to the skeletal muscle was reported to be markedly diminished in diet-induced insulin resistance (Eilmerer et al., 2006). These findings suggest that impairment of insulin delivery, possibly caused by an endothelial insulin signaling defect, may play a critical role in the skeletal muscle insulin resistance seen in obesity.

Why were decreased insulin signaling and decreased glucose uptake in response to insulin observed only in the skeletal muscle of the ETIrs2KO mice and not in their liver? The difference between the types of capillaries in the liver and skeletal muscle may explain these differences in the insulin sensitivity of the two organs. It is thought that the occluded junctions of the endothelial cells of the capillaries in the skeletal muscle may prevent paracellular transport of most macromolecules, including insulin, whereas the fenestrated endothelium of the capillaries in the liver freely permits paracellular passage of macromolecules (Aird, 2007). In fact, more rapid insulin action kinetics have been observed in the liver than in the skeletal muscle (Sherwin et al., 1974).

Insulin-induced phosphorylation of Akt and eNOS in the ETIrs2KO mice was significantly, but not completely, impaired by endothelial Irs2 deficiency (Figure 2D), suggesting the important role of both Irs2 and Irs1 in this signaling in the endothelial cells. In fact, phosphorylation of Akt and eNOS was completely abrogated in the ETIrs1/2DKO mice (Figure 3I). Thus, in the physiological state, it is likely that insulin-stimulated Irs1-mediated Akt activates eNOS in proportion to the amount of eNOS protein available in these mice.

In this study, we found that endothelial insulin signaling mediates insulin-stimulated capillary recruitment and increase of interstitial insulin concentrations and, as a consequence, facilitates glucose uptake by the skeletal muscle. Skeletal muscle insulin resistance may be caused by impaired insulin signaling not only in the myocytes but also in the endothelial cells. Taken together, treatment directed at improving insulin signaling in the endothelial cells as well as myocytes may serve as a therapeutic strategy for ameliorating skeletal muscle insulin resistance.

EXPERIMENTAL PROCEDURES

Mice

ETIrs1KO or ETIrs2KO mice were generated by mating $Irs1^{lox/+}$ or $Irs2^{lox/+}$ female mice (Kubota et al., 2008) with transgenic mice expressing Cre under control of the murine Tie2 promoter (Tie2-Cre mice) (Kisanuki et al., 2001). The $Irs1^{lox/+};Tie2-Cre$ or $Irs2^{lox/+};Tie2-Cre$ male offspring were then crossed with $Irs1^{lox/+}$ or $Irs2^{lox/+}$ female mice to obtain WT ($Irs1^{+/+}$), Tie2-Cre ($Irs1^{+/+};Tie2-Cre$), control ($Irs1^{lox/lox}$), and ETIrs1KO ($Irs1^{lox/lox};Tie2-Cre$) mice, or WT ($Irs2^{+/+}$), Tie2-Cre ($Irs2^{+/+};Tie2-Cre$), control ($Irs2^{lox/lox}$), and ETIrs2KO ($Irs2^{lox/lox};Tie2-Cre$) mice, respectively. To generate endothelial-specific Irs1/Irs2 double-knockout (ETIrs1/2DKO) mice, $Irs1^{lox/+};Tie2-Cre$ or $Irs2^{lox/+};Tie2-Cre$ male mice were crossed with $Irs2^{lox/+}$ or $Irs1^{lox/+}$ female mice, and the resultant $Irs1^{lox/+};Irs2^{lox/+};Tie2-Cre$ male mice were crossed with $Irs1^{lox/+};Irs2^{lox/+}$ female mice. $Irs1^{lox/lox};Irs2^{lox/lox}$ mice were used as the control for ETIrs1/2DKO mice. Only male littermates were used for this study; we did not use the female Tie2-Cre, $Irs1^{lox/+};Tie2-Cre$, $Irs2^{lox/+};Tie2-Cre$, $Irs1^{lox/+};Irs2^{lox/+};Tie2-Cre$, ETIrs1KO, ETIrs2KO, or ETIrs1/2DKO mice for breeding. Further information is provided in the Supplemental Information. The animal care and experimental procedures used in this study were approved by the Animal Care Committee of the University of Tokyo.

Capillary Blood Volume

The capillary blood volume was measured by contrast-enhanced ultrasound, as described previously (Vincent et al., 2004), with some modifications. The hindlimb muscles were imaged in the short axis using a 40 MHz transducer (RMV 704) connected to an ultrasound system (Vevo 770; VISUALSONICS Inc.). Sonazoid (Daiichi Sankyo Corporation) was infused into the animals, which were divided into three groups for the measurements at 0, 10, and 60 min after the hyperinsulinemic-euglycemic clamp, a high-power ultrasound with a frequency of 1MHz was applied to the lower leg muscles, and images were collected for 30 s to assess the enhancement. The ultrasound intensity in decibels within the region of interest was converted to the acoustic intensity after background subtraction using 0.5 s ultrasound images, and the microvascular volume, fill rate constant, and capillary blood volume were calculated according to the equation $y = A(1 - e^{-\beta t})$. Further information is provided in the Supplemental Information.

Interstitial Concentrations of Insulin in the Skeletal Muscle

Muscle microdialysis was performed in the hindlimb muscles using a 4 mm microdialysis tubing (CMA-20) at the rate of 0.3 μ l/min. We conducted calibration using the no-net flux technique described previously (Jansson et al., 1993), with slight modifications. Briefly, four known concentrations of insulin (0 ng/ml, 0.5 ng/ml, 1 ng/ml, and 1.5 ng/ml) above and below the expected concentration in the skeletal muscle were used. The insulin solutions were added to the perfusate, and the net changes in the concentrations of the analytes in the dialysate were recorded ($insulin_{out} - insulin_{in} = net\ change$). Regression analysis yielded a linear relationship between the concentrations in the perfusates and the dialysates. The intercept with the x axis indicates the insulin concentrations in the perfusate at equilibrium with the surrounding medium, and the slope of the line yields the dialysis recovery by the no-net flux technique. The insulin concentrations in the interstitial fluid were calculated from the dialysis recovery by the no-net flux technique and the in vivo dialysate insulin concentration, as described previously (Sjostrand et al., 2002).

Endothelial Cell Culture

The aorta was dissected out from the aortic arch to the abdominal aorta and immersed in 10% FBS-DMEM containing 1000 U/ml heparin. A 24-gauge cannula was inserted into the proximal portion of the aorta. The other side was tied, and the lumen was filled with a solution of collagenase type II (2 mg/ml, dissolved in serum-free DMEM). After incubation at 37°C for 45 min, the endothelial cells were removed from the aorta by flushing with 5 ml of DMEM containing 10% FBS and cultured in a 35 mm collagen type 1-coated dish. Further information is provided in the [Supplemental Information](#).

Hyperinsulinemic-Euglycemic Clamp

An infusion catheter was inserted into the right jugular vein of the mice, as described previously ([Kubota et al., 2008](#)), with some modifications. 1% glucose ([6,6-²H₂]glucose [Sigma]) was infused intravenously, and after a 90 min basal period a blood sample was collected from the tail tip for determination of the basal glucose specific activity. To measure the GIR, a primed-continuous infusion of insulin (Humulin R; Lilly) was administered and the blood glucose concentration was maintained at approximately 120 mg/dl by the administration of glucose (5 g of glucose/10 ml enriched to about 20% with [6,6-²H₂]glucose [Sigma]) for 60 or 120 min. Blood samples (20 μl) were obtained for 15 or 30 min before the end of the hyperinsulinemic-euglycemic clamp. Thereafter, the Rd was calculated according to non-steady-state equations, and the EGP was calculated as the difference between the Rd values and the exogenous GIR. Further information is provided in the [Supplemental Information](#).

Statistical Analysis

Values were expressed as means ± SEM. Student's t test was used for statistical analysis of the differences between two groups, and the statistical significance of differences among multiple groups was determined by ANOVA.

SUPPLEMENTAL INFORMATION

Supplemental Information includes six figures, one movie, Supplemental Experimental Procedures, and Supplemental References and can be found with this article at [doi:10.1016/j.cmet.2011.01.018](https://doi.org/10.1016/j.cmet.2011.01.018).

ACKNOWLEDGMENTS

We thank Namiko Okajima-Kasuga, Sayaka Sasamoto, Kousuke Yokota, Miyoko Suzuki-Nakazawa, Masahiro Nakamaru, Michiko Kato, Tomoko Asano, Eishin Hirata, Eri Yoshida-Nagata, Ayumi Nagano, Miharuru Nakashima, Ritsuko Fujita, and Hiroshi Chiyonobu for their technical assistance and care of the animals. This work was supported by a grant for CREST from the Japan Science and Technology Corporation; a grant for Promotion of Fundamental Studies in Health Science from the Organization for Pharmaceutical Safety and Research; a grant for TSBMI from the Ministry of Education, Culture, Sports, Science and Technology of Japan; a Grant-in-Aid for Scientific Research in Priority Areas (A) (16209030), (A) (18209033), and (S) (20229008) from the Ministry of Education, Culture, Sports, Science, and Technology of Japan (to T. Kadowaki); and a Grant-in-Aid for Scientific Research in Priority Areas (C) (19591037) and (B) (21390279) from the Ministry of Education, Culture, Sports, Science, and Technology of Japan (to N.K.).

Received: May 10, 2010

Revised: August 13, 2010

Accepted: January 24, 2011

Published: March 1, 2011

REFERENCES

Aird, W.C. (2007). Phenotypic heterogeneity of the endothelium. I. Structure, function, and mechanisms. *Circ. Res.* 100, 158–173.

Barrett, E.J., Eggleston, E.M., Inyard, A.C., Wang, H., Li, G., Chai, W., and Liu, Z. (2009). The vascular actions of insulin control its delivery to muscle and

regulate the rate-limiting step in skeletal muscle insulin action. *Diabetologia* 52, 752–764.

Bergman, R.N. (1989). Lilly Lecture: toward physiological understanding of glucose tolerance: minimal-model approach. *Diabetes* 38, 1512–1527.

Brüning, J.C., Michael, M.D., Winnary, J.N., Hayashi, T., Hörsch, D., Accili, D., Goodyear, L.J., and Kahn, C.R. (1998). A muscle-specific insulin receptor knockout exhibits features of the metabolic syndrome of NIDDM without altering glucose tolerance. *Mol. Cell* 2, 559–569.

Chiu, J.D., Richey, J.M., Harrison, L.N., Zuniga, E., Kolk, C.M., Kirkman, E., Ellmerer, M., and Bergman, R.N. (2008). Direct administration of insulin into skeletal muscle reveals that the transport of insulin across the capillary endothelium limits the time course of insulin to activate glucose disposal. *Diabetes* 57, 828–835.

Clark, M.G. (2008). Impaired microvascular perfusion: a consequence of vascular dysfunction and a potential cause of insulin resistance in muscle. *Am. J. Physiol. Endocrinol. Metab.* 295, E732–E750.

DeFronzo, R.A., Tobin, J.D., and Andres, R. (1979). Glucose clamp technique: a method for quantifying insulin secretion and resistance. *Am. J. Physiol.* 237, E214–E223.

Ellmerer, M., Hamilton-Wessler, M., Kim, S.P., Huecking, K., Kirkman, E., Chiu, J., Richey, J., and Bergman, R.N. (2006). Reduced access to insulin-sensitive tissues in dogs with obesity secondary to increased fat intake. *Diabetes* 55, 1769–1775.

Hamilton-Wessler, M., Ader, M., Dea, M.K., Moore, D., Loftager, M., Markussen, J., and Bergman, R.N. (2002). Mode of transcapillary transport of insulin and insulin analog NN304 in dog hindlimb: evidence for passive diffusion. *Diabetes* 51, 574–582.

Jansson, P.A., Fowelin, J.P., von Schenck, H.P., Smith, U.P., and Lönnroth, P.N. (1993). Measurement by microdialysis of the insulin concentration in subcutaneous interstitial fluid. Importance of the endothelial barrier for insulin. *Diabetes* 42, 1469–1473.

Jiang, Z.Y., Lin, Y.W., Clemont, A., Feener, E.P., Hein, K.D., Igarashi, M., Yamauchi, T., White, M.F., and King, G.L. (1999). Characterization of selective resistance to insulin signaling in the vasculature of obese Zucker (*fa/fa*) rats. *J. Clin. Invest.* 104, 447–457.

Kainoh, M., Maruyama, I., Nishio, S., and Nakadate, T. (1991). Enhancement by beraprost sodium, a stable analogue of prostacyclin, in thrombomodulin expression on membrane surface of cultured vascular endothelial cells via increase in cyclic AMP level. *Biochem. Pharmacol.* 41, 1135–1140.

Karnieli, E., Zarnowski, M.J., Hissin, P.J., Simpson, I.A., Salans, L.B., and Cushman, S.W. (1981). Insulin-stimulated translocation of glucose transport systems in the isolated rat adipose cell. Time course, reversal, insulin concentration dependency, and relationship to glucose transport activity. *J. Biol. Chem.* 256, 4772–4777.

Keske, M.A., Clerk, L.H., Price, W.J., Jahn, L.A., and Barrett, E.J. (2009). Obesity blunts microvascular recruitment in human forearm muscle after a mixed meal. *Diabetes Care* 32, 1672–1677.

Kisanuki, Y.Y., Hammer, R.E., Miyazaki, J., Williams, S.C., Richardson, J.A., and Yanagisawa, M. (2001). Tie2-Cre transgenic mice: a new model for endothelial cell-lineage analysis in vivo. *Dev. Biol.* 230, 230–242.

Kubota, T., Kubota, N., Moroi, M., Terauchi, Y., Kobayashi, T., Kamata, K., Suzuki, R., Tobe, K., Namiki, A., Aizawa, S., et al. (2003). Lack of insulin receptor substrate-2 causes progressive neointima formation in response to vessel injury. *Circulation* 107, 3073–3080.

Kubota, N., Kubota, T., Itoh, S., Kumagai, H., Kozono, H., Takamoto, I., Mineyama, T., Ogata, H., Tokuyama, K., Ohsugi, M., et al. (2008). Dynamic functional relay between insulin receptor substrate 1 and 2 in hepatic insulin signaling during fasting and feeding. *Cell Metab.* 8, 49–64.

Long, Y.C., and Zierath, J.R. (2008). Influence of AMP-activated protein kinase and calcineurin on metabolic networks in skeletal muscle. *Am. J. Physiol. Endocrinol. Metab.* 295, E545–E552.

Miles, P.D., Levisetti, M., Reichart, D., Khoursheed, M., Moossa, A.R., and Olefsky, J.M. (1995). Kinetics of insulin action in vivo. Identification of rate limiting steps. *Diabetes* 44, 947–953.

- Muniyappa, R., and Quon, M.J. (2007). Insulin action and insulin resistance in vascular endothelium. *Curr. Opin. Clin. Nutr. Metab. Care* 10, 523–530.
- Niwano, K., Arai, M., Tomaru, K., Uchiyama, T., Ohyama, Y., and Kurabayashi, M. (2003). Transcriptional stimulation of the eNOS gene by the stable prostacyclin analogue beraprost is mediated through cAMP-responsive element in vascular endothelial cells: close link between PGI₂ signal and NO pathways. *Circ. Res.* 93, 523–530.
- Nolan, J.J., Ludvik, B., Baloga, J., Reichart, D., and Olefsky, J.M. (1997). Mechanisms of the kinetic defect in insulin action in obesity and NIDDM. *Diabetes* 46, 994–1000.
- Petersen, K.F., Dufour, S., Befroy, D., Garcia, R., and Shulman, G.I. (2004). Impaired mitochondrial activity in the insulin-resistant offspring of patients with type 2 diabetes. *N. Engl. J. Med.* 350, 664–671.
- Rattigan, S., Clark, M.G., and Barrett, E.J. (1997). Hemodynamic actions of insulin in rat skeletal muscle: evidence for capillary recruitment. *Diabetes* 46, 1381–1388.
- Sherwin, R.S., Kramer, K.J., Tobin, J.D., Insel, P.A., Liljenquist, J.E., Berman, M., and Andres, R. (1974). A model of the kinetics of insulin in man. *J. Clin. Invest.* 53, 1481–1492.
- Sjostrand, M., Gudbjornsdottir, S., Holmang, A., Lonn, L., Strindberg, L., and Lönnroth, P. (2002). Delayed transcapillary transport of insulin to muscle interstitial fluid in obese subjects. *Diabetes* 51, 2742–2748.
- Vicent, D., Ilany, J., Kondo, T., Naruse, K., Fisher, S.J., Kisanuki, Y.Y., Bursell, S., Yanagisawa, M., King, G.L., and Kahn, C.R. (2003). The role of endothelial insulin signaling in the regulation of vascular tone and insulin resistance. *J. Clin. Invest.* 111, 1373–1380.
- Vincent, M.A., Clerk, L.H., Lindner, J.R., Klibanov, A.L., Clark, M.G., Rattigan, S., and Barrett, E.J. (2004). Microvascular recruitment is an early insulin effect that regulates skeletal muscle glucose uptake in vivo. *Diabetes* 53, 1418–1423.
- Vincent, M.A., Clerk, L.H., Rattigan, S., Clark, M.G., and Barrett, E.J. (2005). Active role for the vasculature in the delivery of insulin to skeletal muscle. *Clin. Exp. Pharmacol. Physiol.* 32, 302–307.
- Wallis, M.G., Wheatley, C.M., Rattigan, S., Barrett, E.J., Clark, A.D.H., and Clark, M.G. (2002). Insulin-mediated hemodynamic changes are impaired in muscle of Zucker obese rats. *Diabetes* 51, 3492–3498.
- Wang, H., Wang, A.X., Liu, Z., and Barrett, E.J. (2008). Insulin signaling stimulates insulin transport by bovine aortic endothelial cells. *Diabetes* 57, 540–547.
- White, M.F., and Kahn, C.R. (1994). The insulin signaling system. *J. Biol. Chem.* 269, 1–4.
- Yang, Y.J., Hope, I.D., Ader, M., and Bergman, R.N. (1989). Insulin transport across capillaries is rate limiting for insulin action in dogs. *J. Clin. Invest.* 84, 1620–1628.